ACADEMIA ROMÂNĂ
Revue Roumaine de Chimie
https://www.icf.ro/rrch/

Rev. Roum. Chim.,
2026, *71*(5–6), 325–332
DOI: 10.33224/rrch.2026.71.5-6.03

Dedicated to Professor Alexandru T. Balaban on the occasion of his 95th anniversary

THE SYNTHESIS and STRUCTURAL CHARACTERIZATION OF A NEW IODINATED STRIGOLACTONE MIMIC**

Florea DUMITRASCU,[a] Sergiu SHOVA,[b] Florentina GEORGESCU,[c*]
Constantin DRAGHICI[a] and Marcel Mirel POPA[a*]

[a] C. D. Nenitescu Institute of Organic and Supramolecular Chemistry, Roumanian Academy, 202 B, Splaiul Independentei, 060023 Bucharest, Roumania
[b] Petru Poni Institute of Macromolecular Chemistry, Romanian Academy, Aleea Grigore Ghica Voda 41A, 700487 Iasi, Roumania
[c] Enpro Soctech Com srl, Str. Elefterie 51, 050524 Bucharest, Roumania

Received December 2, 2025

Herein is presented the synthesis of a new strigolactone mimic with an iodine atom in view of the future investigation of how the halogen atoms influence physico-chemical or biological properties of such compounds. The title compound was synthesized in good yield and structurally characterized by NMR spectroscopy and single-crystal X-ray diffraction. Compound **3** crystal packing is directed by weak H···O bonds and an important I···O halogen contact.

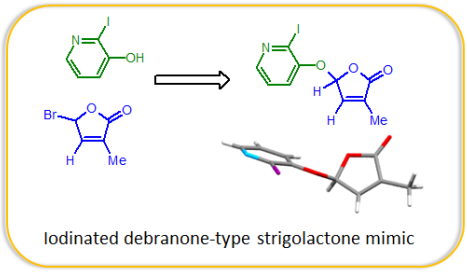

INTRODUCTION

Strigolactone is the generic name of a group of naturally carotenoid derived allelochemicals with complex functions in plant biology. Until now over 25 naturally occurring strigolactones have been isolated in tiny amounts from the exudates of various mono- and dicotyledonous plants. These compounds display a large range of biological activities. Thus, they act as signalling molecules in the rhizosphere controlling the germination of parasitic weed seeds,[1–7] hyphal branching in arbuscular mycorrhizal (AM) fungi,[8–11] phytohormones involved in plants development,[12–21] and in plants responses to both biotic and abiotic stresses.[22,23] The complex structures of naturally occurring strigolactones have a tricyclic lactone core system (ABC) connected through an enol-ether bond to a furan-2-one ring. Strigolactones have been classified into canonical and non-canonical structures.[24–26] In the canonical strigolactones the ABC-ring system, the D-ring and the enol-ether

* Corresponding author: mirelupb@gmail.com (M.M.P.); florentina_fg@yahoo.com (F.G.)
** Supplementary information on https://www.icf.ro/rrch/ or htts://revroum.lew.ro

bond acting as a connection of the two parts are present. Based on stereochemistry canonical strigolactones have been classified into two major groups: one having the parent structure of strigol and the other one with the parent structure of orobanchol (Fig. 1).

In the non-canonical strigolactone-like compounds the A, B, or/and C rings are replaced by a carotenoid-type structure, but the D-ring and the enol-ether bridge are present, these two parts being the common feature of both canonical and non-canonical strigolactones.[24–26]

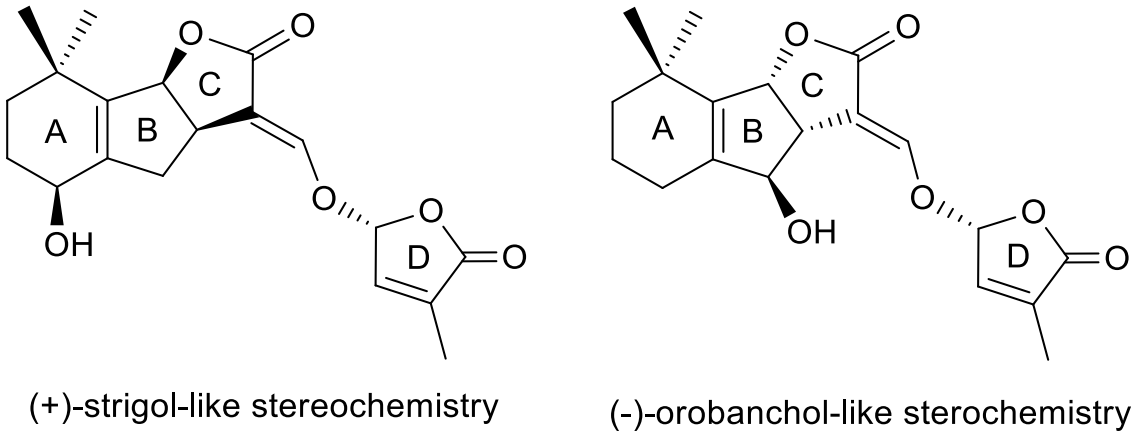

Fig. 1 – Naturally occurring canonical strigolactones,

The complex structures of naturally strigolactones and their laborious multi-step synthesis encouraged the synthesis of simplified molecules leading to novel synthetic strigolactone analogues and mimics showing their various bioactivities. Strigolactones bioactivities are not affected by the structural changes of A, B and even C rings or by the replacement of an oxygen atom by the nitrogen atom as in imino strigolactone analogues,[27] or strigolactam analogues.[28] Usually, synthetic strigolactone analogues contain the bioactiphore CD part of natural compounds, while strigolactone mimics have the D-ring directly linked to aroyloxy, (het)aryloxy, or even heteroaryl moieties. A large group of strigolactone analogues and mimics, including the so-called debranones which have a (het)aryl substituent connected directly to the furan-2-one D ring through an ether or thioether link, showed remarkable phytohormone bioactivity,[12-21] and interesting medicinal properties.[29–31]

In the last years, our group was interested in syntheses of novel simplified synthetic strigolactone analogues and mimics, accessible in significant amounts and their biological and photophysical properties were investigated.[32–38] Their promising applications as plant and microalgae biostimulants,[32–37] fluorescent cell markers or chemosensors for water detection in organic media have been reported.[38] Continuing our interest in the field of bioactive compounds we have synthesized an iodinated strigolactone mimic starting from 2-iodo-3-hydroxypyridine in order to investigate the influence of the iodine on the bioavailability of the new strigolactone mimic. Herein we present the synthesis of the new strigolactone mimic 5-[(2-iodopyridin-3-yl)oxy]-3-methylfuran-2(5*H*)-one, structurally characterized by NMR spectroscopy, the single-crystal X-ray diffraction and Hirshfeld surface analysis.

RESULTS AND DISCUSSION

A potentially bioactive strigolactone mimic was obtained by the coupling reactions of 2-iodopyridin-3-ol **1** in acetone with freshly prepared 5-bromo-3-methyl-5*H*-furan-2-one **2**, in the presence of potassium carbonate as basic catalyst, led to the desired strigolactone mimic 5-[(2-iodopyridin-3-yl)oxy]-3-methylfuran-2(5*H*)-one **3** in good yield (Scheme 1). The compound 5-bromo-3-methylfuran-2(5*H*)-one **2** was prepared by the bromination of 3-methyl-5*H*-furan-2-one with *N*-bromosuccinimide in the presence of catalytic amounts of a radical initiator such as dibenzoyl peroxide or 2,2′-azobis(isobutyronitrile).[39]

The compound was synthesized and fully structural characterized by ^{1}H and ^{13}C NMR (Figs. 1S and 2S – Supplementary Material) spectroscopy, ATR-IR and by single-crystal X-ray diffraction.

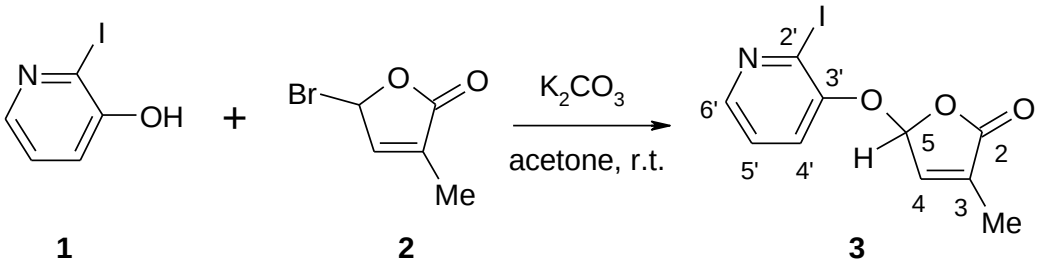

1 **2** **3**

Scheme 1 – Synthesis of 5-[(2-iodopyridin-3-yl)oxy]-3-methylfuran-2(5*H*)-one **3**.

In the ^{1}H NMR spectrum the signals of the two protons H-4 and H-5 from furanone ring appear as two quintets. The multiplicity of H-4 and H-5 is explained by the coupling of these protons both to each other and to the protons of the methyl group. The protons in the methyl group are coupled to H-4 and H-5 and their signal appears as a triplet at 2.05 ppm. The three protons in the pyridine ring are coupled to each other have large chemical shifts presenting as an AMX spin system, with doublet of doublets multiplicities.

The ^{13}C NMR spectrum show all expected signals. The chemical shifts of the carbon atoms in the furanone ring were assigned based on NMR experiments such as HETCOR. The most deshielded carbon atom signal appears at 170.8 ppm and corresponds to the lactonic C=O of the furanone group. The signal of C_{sp3} (C-5) in the furanone ring has a chemical shift of 99.7 ppm whereas the two carbon atoms of the double C=C bond (C-3 and C-4) are more deshielded and their resonance signals appear at 135.3 ppm and 141.3 ppm. The chemical shifts of carbon atoms from pyridine moiety are strongly influenced by electronic effects. Thus, the carbon atom having attached iodine atom (C-2') is the most shielded and has is resonance at 113.2 ppm whereas C-3'(δ=153.0 ppm) and C-6' (δ=146.2 ppm) are strongly deshielded by electronic effects of the adjacent oxygen atom which is attached to C-3' and of the neighboring nitrogen atom.

The most distinctive peak in the IR spectrum is the strong C=O stretch band which has a wavenumber of 1778 cm^{-1} and is characteristic for a lactone functional group.

The single crystal X-ray study has demonstrated that the compound **3** crystallize in $P2_1/c$ space group of monoclinic system with one molecule in the asymmetric unit. A view of the molecular structure is shown in Fig. 2. The values of the bond distances and angles are summarized in Table 1S. The analysis of the crystal packing has revealed the presence of C1-I1···O3^{i} halogen bond (C1-I1 = 2.11, I1···O3 = 3.25 Å, ∠C1I1O3 = 173°, symmetry code: (i) 2–*x*, *y*–0.5, 1.5–*z*), which links adjacent molecules into one-dimensional array running along *b* axis. On the other hand, the pyridine moiety is also involved in hydrogen bond with iodine atom C5-H5···I1 = 3.22 Å (C5-H5 = 0.93 Å, ∠C5H5I1 = 140°) creating another supramolecular chains oriented in perpendicular direction along *c* axis, giving rise for two-dimensional supramolecular wave-like layer extended in *bc* plane, as illustrated in Fig. 3. In turn, 2D layers are further interacting *via* C4-H4···O3^{i} hydrogen bond (C4-H4 = 0.93 Å, H4···O3 = 2.66 Å, ∠C4H4O3 = 146°, symmetry code (i) 1–*x*,1–*y*,1–*z*), which generates a tree-dimensional supramolecular network. A view of this network along *c* axis is illustrated in Fig. 4.

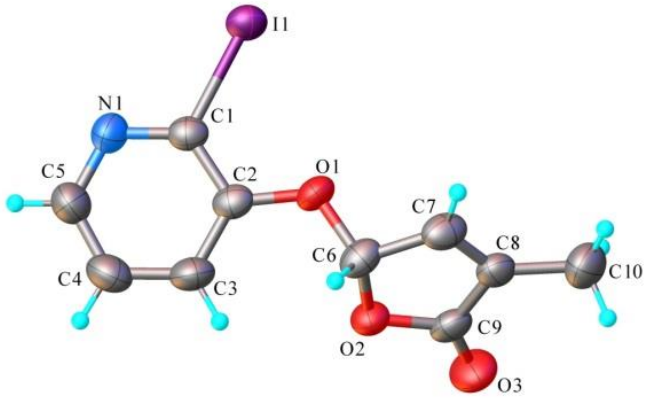

Fig. 2 – X-ray molecular structure of compound **3** with atom labelling and thermal ellipsoids at 50% probability level.

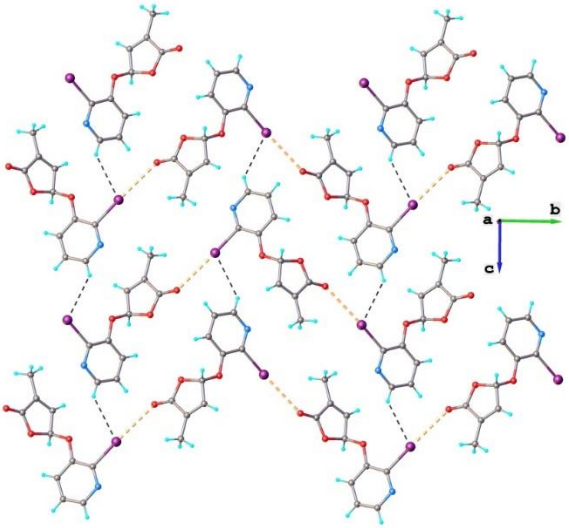

Fig. 3 – View of two-dimensional supramolecular layer in the crystal **3**. Hydrogen and halogen bonds are shown as dotted lines with black and orange color, respectively.

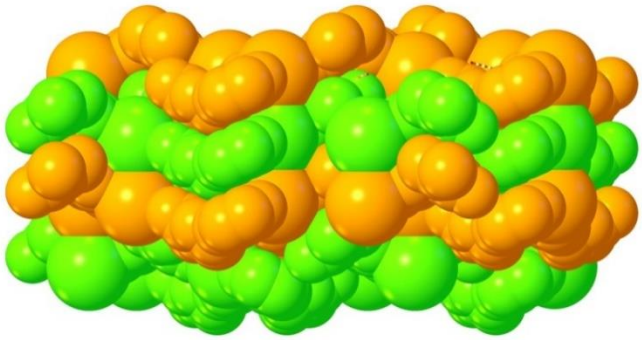

Fig. 4 – A sphere packing representation of the crystal structure **3** viewed along *c* axis, showing the packing of 2D supramolecular layers bonded through C4-H4···O3 contacts.

The Hirshfeld surface confirms the most important contacts in the crystal packing of compound **3**. Figure 5 highlights the HF surface generated on a centered molecule with I···O halogen contacts[40–48] generating infinite arrays and bonding enantiomers in a R-S-R-S model (C-6 chiral center). In the same time centrosymmetric dimers formed by reciprocal H4···O3 contacts are formed between same enantiomers generating parallel arrays of I···O contacts along c-axis.

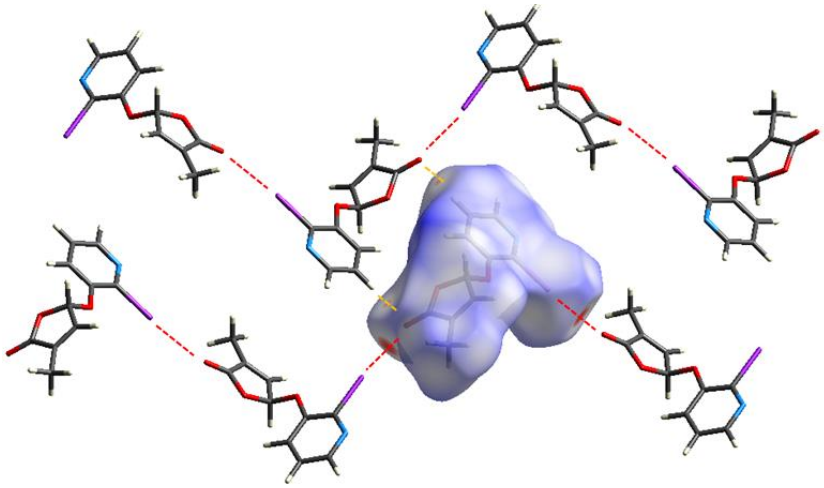

Fig. 5 – Hirshfeld surface generated on one molecule highlighting the most important contacts below the sum of vdW radii and highlighting inifinite I···O arrays interconnected through H···O weak bonds (red spots on the HF surface).

The fingerprint plots (Fig. 6) present the percentage interactions in the crystal packing of three in a quantitative way. The molecular packing is dominated by O···H contacts accounting for 26.1 per cents. I···O contacts account for 5.0 per cents which is rather high and confirm the importance of the halogen I···O bond.

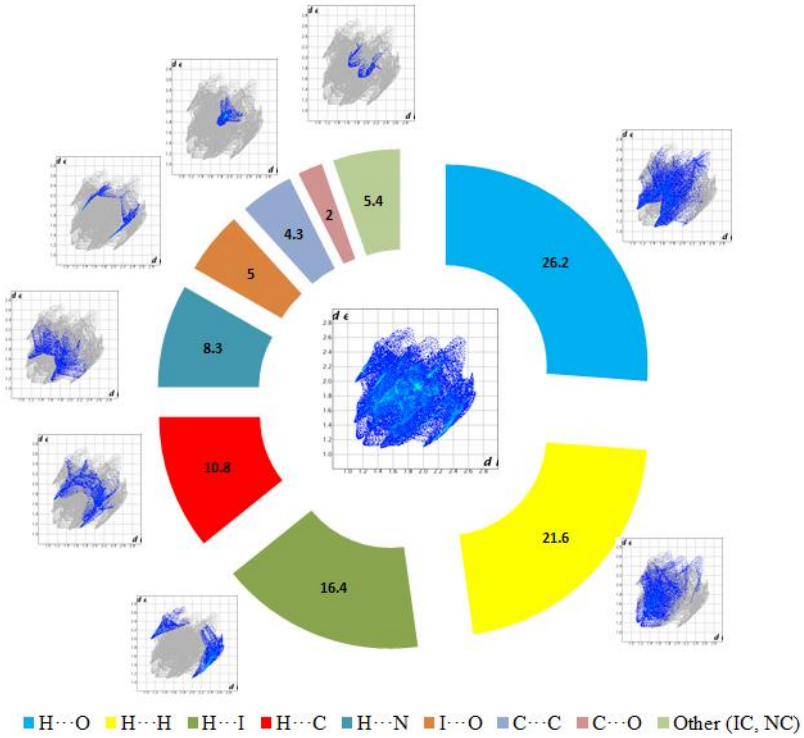

Fig. 6 – Hirshfeld surface derived percentage interaction in the crystal packing of compound **3**.

A closer investigation of the fingerprint plots interactions prompted to investigate the rather high percentage of C···C contacts and other (NC for example) which might infer presence of pi stacking. Even the shape index of the HF surface presented complementarity areas the high ring to ring distance of > 4 Å exclude such interactions. However C···O contacts of 2% led us to investigate a possible lp···π (lp-lone pair) contact between the carbonyl C9=O3 and the furanone ring with a distance O···Cg of 3.617(5) Å and an angle C9O3Cg 85.2(3)° (Fig. 7) which can be included in a carbonyl-π type.[49]

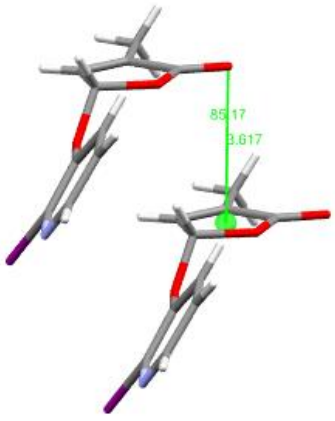

Fig. 7 – Lp···π possible contact between the lactone carbonyl and furanone ring.

EXPERIMENTAL

Synthesis of 5-[(2-iodopyridin-3-yl)oxy]-3-methylfuran-2(5*H*)-one (3)

Melting point, determined on a Boetius apparatus, is uncorrected. The IR spectrum was registered on a Fourier-transform (FT)-IR Vertex 70 spectrometer (Bruker Optik GmbH, Ettlingen, Germany) in ATR modes. The NMR spectra were recorded on a Varian Gemini 300 BB instrument, at 300.1 MHz and 75.5 MHz for ^{1}H and ^{13}C nuclei respectively. Chemical shifts are reported as δ (ppm) and are referenced to internal TMS for ^{1}H chemical shifts and to the internal deuterated solvent for ^{13}C chemical shifts ($CDCl_3$ referenced at 77.0 ppm). The elemental analysis was carried out on a COSTECH Instruments EAS32 apparatus and satisfactory microanalyses were obtained. The 5-bromo-3-methyl-5*H*-furan-2-one **2** was obtained in good yield by the bromination of commercial 3-methyl-5*H*-furan-2-one, technical grade, with *N*-bromosuccinimide in carbon tetrachloride, at reflux, in the presence of catalytic amounts of dibenzoyl peroxide or 2,2′-azobis(isobutyronitrile) and was used as crude reaction product (94-95 %).[39] All reagents and solvents were commercially products (Sigma-Aldrich) and have been used without purification.

***5-[2-Iodopyridin-3-yl)oxy]-3-methylfuran-2(5H)-one* (3)**: to a solution of g (10) mmol of 2-iodopyridin-3-ol **1** in 20 mL acetone 2.1 g (15 mmol) anhydrous potassium carbonate was added, then 2.4 g (15 mmol) of crude 5-bromo-3-methyl-5*H*-furan-2-one **2** dissolved in 20 mL of acetone was slowly added under stirring at room temperature. The stirring was continued for 24 hours at room temperature and the reaction mixture was filtered off to remove the inorganic impurities. After the removal of the acetone the residue was chromatographed on an alumina 70–230 mesh packed column by eluting with dichloromethane and the desired compound **3** was isolated and crystallized from EtOH (1.97 g, yield 62%), mp 122–124 ºC. Anal. Calcd. for $C_{10}H_8INO_3$ (317.08): C, 37.88; H, 2.54; N, 4.42. Found: C, 37.93; H, 2.50; N, 4.48. ATR-FTIR (solid): 1778, 1667, 1559, 1444, 1409, 1353, 1263, 1200, 1135, 1084, 1008, 955 cm^{-1}. ^{1}H NMR ^{1}H NMR (300 MHz, $CDCl_3$), δ (ppm): 2.05 (t, 3H, Me) 6.21 (quint., 1H, H-5), 7.12 (quint., 1H, H-4), 7.26 (dd, 1H, *J*=8.2, 4.4 Hz, H-5'), 7.48 (dd, 1H, *J*=8.2, 1.8 Hz, H-4'), 8.17 (dd, 1H, *J*=4.4, 1.8 Hz, H-6'); ^{13}C-NMR (75 MHz, $CDCl_3$), δ (ppm): 10.8 (Me), 99.7 (C-5), 113.2 (C-2'), 123.8, 124.1, 146.2 (C-4', C-5', C-6'), 135.3 (C-4), 141.8 (C-3), 153.0 (C-3'), 170.8 (CO).

Single-crystal X-ray diffraction

Single-crystal X-ray diffraction data for compound **3** were collected with an XtaLAB Synergy, Dualflex, HyPix diffractometer using Cu Kα radiation. The unit cell determination and data integration were carried out using the CrysAlisPro package from Oxford Diffraction.[50] The structure was solved with SHELXT program using the intrinsic phasing method and refined by the full-matrix least-squares method on F^2 with SHELXL.[51,52] Olex2 was used as an interface to the SHELX programs.[53] Non-hydrogen atoms were refined anisotropically. Hydrogen atoms were added in idealized positions and refined using a riding model. The molecular plots were obtained with the Olex2 program. Selected crystallographic data and structure refinement details are provided in Table 1 (specific bond lengths and angles are presented in Table 1S – Supplemmentary Material) and the corresponding CIF-file. Deposition Number **2503200** contains the supplementary crystallographic data for this paper. These data are provided free of charge by the joint Cambridge Crystallographic Data Centre and Fachinformationszentrum Karlsruhe http://www.ccdc.cam.ac.uk/structures

Table 1

Crystallographic data and refinement details for compound **3**

Empirical formula	$C_{10}H_8INO_3$
Formula weight	317.07
Temperature/K	293
Space group	$P2_1/c$
a/Å	4.12978(18)
b/Å	17.8275(7)
c/Å	14.7549(7)
α/°	90
β/°	91.241(4)
γ/°	90
Volume/Å^3	1086.05(8)
Z	4
ρ_{calc}g/cm^3	1.939
μ/mm^{-1}	2.934
Crystal size/mm^3	0.20×0.15×0.03
2Θ range/°	4.57 to 50.044
Refs collected	6264
Indep. refls	1884, 0.0310
Data/restrs/params	1884/0/137
GOF on F^2	1.041
R_1, wR_2(all data)	0.0378, 0.0830

Hirshfeld analysis

Hirshfeld analysis was performed using the Crystal Explorer 17 package.[54,55] Hirshfeld surfaces were defined at the distance between the interior and exterior atoms involved in different contacts and depicted with red colour for contacts less than the sum of the van der Waals (vdW) radii of the specific atoms, white colour at the sum of the vdW radii and blue colour for longer distances.[54] Fingerprint plots[55] were defined as percentage interactions extracted from the Hirshfeld surfaces.

CONCLUSIONS

A new potentially active debranone-like strigolactone mimic 5-[(2-iodopyridin-3-yl)oxy]-3-methylfuran-2(5*H*)-one was synthesized and structurally characterized by NMR and the single-crystal X-ray diffraction. Presence of iodine atom in compound **3** led to I···O halogen contacts which are the most important in the crystal packing along with weak H-bond of type C-H··O or C-H···I. The presence of the large polarisable iodine atom could influence the bioavailability of the compound **3**.

REFERENCES

1. C. E. Cook, L. P. Whichard, B. Turner, M. E. Wall and G. H. Egley, *Science* **1966**, *154*, 1189–1190.
2. C. E. Cook, P. Coggon, A. T. McPhail, M. E. Wall, L. P. Whichard, G. H. Egley and P. A. Luhan, *J. Am. Chem. Soc.* **1972**, *94*, 6198–6199.
3. E. M. Mangnus and B. Zwanenburg, *J. Agric. Food Chem.* **1992**, *40*, 1066–1070.
4. R. Matusova, K. Rani, F. W. A. Verstappen, M. C. R. Franssen, M. H. Beale and H. J. Bouwmeester, *Plant Physiol.* **2005**, *139*, 920–934.
5. K. Yoneyama, X. Xie, K. Yoneyama and Y. Takeuchi, *Pest. Manag. Sci.* **2009**, *65*, 467–470.
6. B. Zwanenburg, A. S. Mwakaboko, A. Reizelman, G. Anilkumar and D. Sethumadhavan, *Pest. Manag. Sci*. **2009**, *65*, 478–491.
7. X. Xie, K. Yoneyama and K.Yoneyama, *Annu. Rev. Phytopathol.* **2010**, *48*, 93–117.
8. K. Akiyama, K.-I. Matsuzaki and H. Hayashi, *Nature* **2005**, *435*, 824–827.
9. H. J. Bouwmeester, C. Roux, J. A. Lopez-Raez and G. Becard, *Trends Plant Sci.* **2007**, *12*, 224–230.
10. K. Akiyama, S. Ogasawara, S. Ito and H. Hayashi, *Plant Cell Physiol.* **2010**, *51*, 1104–1117.
11. A. Besserer, V. Puech-Pages, P. Kiefer, V. Gomez-Roldan, A. Jauneau, S. Roy, J. C. Portais, C. Roux, G. Becard and N. Sejalon-Delmas, *PLoS Biol.* **2006**, *4*, 1239–1247.
12. V. Gomez-Roldan, S. Fermas, P. B. Brewer, V. Puech-Pagčs, E. A. Dun, J.-P. Pillot, F. Letisse, R. Matusova, S. Danoun, J.-C. Portais, H. J. Bouwmeester, G. Bécard, C. A. Beveridge, C. Rameau and S. F. Rochange, *Nature* **2008**, *455*, 189–194.
13. F.-D. Boyer, A. de Saint Germain, J.-P. Pillot, J.-B. Pouvreau, V. X. Chen, S. Ramos, A. Stevenin, P. Simier, P. Delavault, J.-M. Beau and C. Rameau, *Plant Physiol*. **2012**, *159*, 1524–1544.
14. P. B. Brewer, H. Koltai and C. A. Beveridge, *Mol. Plant* **2013**, *6*, 18–28.
15. B. Zwanenburg and T. Pospíšil, *Mol. Plant* **2013**, *6*, 38–62.
16. S. Al-Babili and H. J. Bouwmeester, *Annu. Rev. Plant Biol.* **2015**, *66*, 161–186.
17. B. Zwanenburg, T. Pospíšil and Ć. S. Zeljković, *Planta* **2016**, *243*, 1311–1326.
18. C. Rameau, S. Goormachtig, F. Cardinale, T. Bennett and P. Cubas, Strigolactones – Biology and Applications, Springer, H. Koltai, C. Prandi, Eds., **2019**, pp. 47–87.
19. H. J. Bouwmeester, R. Fonne-Pfister, C. Screpanti and A. De Mesmaeker, *Angew. Chem. Int. Ed*. **2019**, *58*, 12778–12786.
20. A. Cala, K. Ghooray, M. Fernández-Aparicio, J. M. Molinillo, J. C. Galindo, D. Rubiales and F. A. Macías, *Pest. Manag. Sci*. **2016,** *72*, 2069–2081.
21. M. Dvorakova, P. Soudek and T. Vanek, *J. Nat. Prod*. **2017**, *80*, 1318–1327.
22. Y. Kapulnik and H. Koltai, *Planta Physiol.* **2014**, *166*, 560–569.
23. C. Screpanti, R. Fonné-Pfister, A. Lumbroso, S. Rendine, M. Lachia and A. de Mesmaeker, *Bioorg. Med. Chem. Lett.* **2016**, *26*, 2392–2400.
24. K. P. Jia and S. Al-Babili, *J. Exp. Bot.* **2018**, *69*, 2189–2204
25. Y. Wang and H. J. Bouwmeester, *J. Exp. Bot*. **2018**, *69*, 2219–2230.
26. K. Yoneyama, X. Xie, K. Yoneyama, T. Kisugi, T. Nomura, Y. Nakatani, K. Akiyama and C. S. P. McErlean, *J. Exp. Bot.* **2018**, *69*, 2231–2239.
27. Y. Kondo, E. Tadokoro, M. Matsuura, K. Iwasaki, Y. Sugimoto, H. Miyake, H. Takikawa and M. Sasaki, *Biotechnol. Biochem.* **2007**, *71*, 2781–2786.
28. M. Lachia, H. C. Wolf, P. J. M. Jung, C. Screpanti and A. De Mesmaeker, *Bioorg*. *Med*. *Chem*. *Lett*. **2015**, *25*, 2184–2188.
29. P. Carrillo, B. Martınez-Poveda, M. A. Medina and A. R. Quesada, *Biochem. Pharmacol.* **2019**, *168*, 366–383.
30. V. Dell'Oste, F. Spyrakis and C. Prandi, *Molecules* **2021**, *26*, 4579.
31. C. Prandi, Y. Kapulnik and H. Koltai, *Eur. J. Org. Chem.* **2021**, 4019–4026.
32. F. Oancea, E. Georgescu, R. Matusova, F. Georgescu, A. Nicolescu, I. Raut, M.-L. Jecu, M.-C. Vladulescu, L. Vladulescu and C. Deleanu, *Molecules* **2017**, *22*, 961.
33. I. Bala, A. Airinei, E. Georgescu, F. Oancea, F. Georgescu, A. Nicolescu, R. Tigoianu and C. Deleanu, *Rev. Roum. Chim*., **2022**, *67*, 51–62.
34. D. G. Popa, F. Georgescu, F. Dumitrascu, S. Shova, D. Constantinescu-Aruxandei, C. Draghici, L. Vladulescu and F. Oancea, *Molecules* **2023**, *28*, 7059.
35. I. A. Bala, A. Nicolescu, F. Georgescu, F. Dumitrascu, A. Airinei, R. Tigoianu, E. Georgescu, D. Constantinescu-Aruxandei, F. Oancea and C. Deleanu, *Molecules* **2024**, *29*, 2283.
36. M. M. Iftime, A. Nicolescu, F. Oancea, F. Georgescu and L. Marin, *Carbohydr. Polym.* **2024**, *144*, 122524–122534.
37. D. Popa, N. Tritean, F. Georgescu, C. Lupu, S. Shaposhnikov, D. Constantinescu-Aruxandei and F. Oancea, *Plants*, **2025**, *14*, 1010.

38. R. Tigoianu, A. Airinei, E. Georgescu, A. Nicolescu, F. Georgescu, D. L. Isac, C. Deleanu and F. Oancea, *Int. J. Mol. Sci.* **2022**, *23*, 2760.
39. G. Macalpine, R. Raphael, A. Shaw, A. Taylor and H. J. Wild, *J. Chem. Soc.-Perkin Trans*. 1, **1976**, 410–416.
40. M. M. Popa, S. Shova, M. Dascalu, M. R. Caira and F. Dumitrascu, *CrystEngComm*, **2023**, *25*, 86–94.
41. M. M. Popa, S. Shova, I. C. Man, and F. Dumitrascu, *J. Mol. Struct.*, **2025**, *1319*, 129384.
42. M. M. Popa, D. G. Dumitrescu, S. Shova, I. C. Man, A. van der Lee and F. Dumitrascu, *J. Mol. Struct.*, **2023**, *1292*, 136112.
43. M. M. Popa, I. C. Man, S. Shova, M. R. Caira, F. Dumitrascu, D. Dumitrescu, *CrystEngComm*, **2019**, *21*, 7085–7093.
44. D. Dumitrescu, S. Shova, I. C. Man, M. R. Caira, M. M. Popa, F. Dumitrascu, *Crystals* **2020**, *10*, 1149.
45. F. Dumitrascu, A.-M. Udrea, M. R. Caira, D. C. Nuta, C. Limban, M. C. Chifiriuc, M. Popa, C. Bleotu, A. Hanganu, D. Dumitrescu, S. Avram, *Molecules* **2022**, *27*, 2722.
46. D. Dumitrescu, S. Shova, C. Draghici, M. M. Popa, F. Dumitrascu, *Molecules* **2021**, *26*, 3693.
47. F. Dumitrascu, M. R. Caira, S. Avram, C. Buiu, A. M. Udrea, I. M. Vlad, I. Zarafu, P. Ionita, D. C. Nuta, M. Popa, M. C. Chifiriuc, *Front. Cell. Infect. Microbiol*. **2023**, *13*, 1181516.
48. C. Draghici, M. R. Caira, D. E. Dumitrescu, F. Dumitrascu, *Rev Chem.* **2018**, *69*, 843–845.
49. M. Egli, S. Sarkhel *Acc. Chem. Res.* **2007**, *40*, 197–205.
50. Rigaku Oxford Diffraction (2015), CrysAlisPro Software system, version 1.171.44.128, Rigaku Corporation, Oxford, UK.
51. G. Sheldrick, SHELXT – Integrated space-group and crystal-structure determination, Acta Cryst. **2015**, *A71*, 3–8.
52. G. Sheldrick, Crystal structure refinement with SHELXT. *Acta Cryst.* **2015**, *C71*, 3–8.
53. O. V. Dolomanov, L. J. Bourhis, R. J. Gildea, J. A. K. Howard and H. Puschmann, OLEX2: a complete structure solution, refinement and analysis program, *J. Appl. Cryst.* **2009**, *42*, 339–341.
54. M.A. Spackman, D. Jayatilaka, *CrystEngComm* **2009**, *11*, 19–32.
55. P.R Spackman, M.J. Turner, J.J. McKinnon, S.K. Wolff, D.J. Grimwood, D. Jayatilaka, M.A. Spackman, *J. Appl. Crystallogr.* **2021**, *54*, 1006–1011.